RR-57

ISSN 0252-1075
Research Report No. RR-057

Contributions from
Indian Institute of Tropical Meteorology

IDENTIFICATION OF SELF-ORGANIZED CRITICALITY IN ATMOSPHERIC TOTAL OZONE VARIABILITY

by

A.M. SELVAM

and

M. RADHAMANI

PUNE - 411 008
INDIA
JULY 1993

ABSTRACT

RR-57

Abstract Long-range spatio-temporal correlations manifested as the self-similar fractal geometry to the spatial pattern concomitant with inverse power law form for the power spectrum of temporal fluctuations are ubiquitous to real world dynamical systems and are recently identified as signatures of self-organized criticality. Self-organized criticality in atmospheric flows is exhibited as the fractal geometry to the global cloud cover pattern and the inverse power law form for the atmospheric eddy energy spectrum. In this paper a recently developed cell dynamical system model for atmospheric flows is summarized. The model predicts inverse power law form of the statistical normal distribution for atmospheric eddy energy spectrum as a natural consequence of quantum-like mechanics governing atmospheric flows extending upto stratospheric levels and above. Model predictions are in agreement with continuous periodogram analyses of atmospheric total ozone. Atmospheric total ozone variability (in days) exhibits the temporal signature of self-organized criticality, namely, inverse power law form for the power spectrum. Further, the long-range temporal correlations implicit to self-organized criticality can be quantified in terms of the universal characteristics of the normal distribution. Therefore, the total pattern of fluctuations of total ozone over a period of time is predictable.

1. INTRODUCTION

Atmospheric total columnar ozone exhibits nonlinear variability on all time scales from days to years (WMO, 1985; GAO and STANFORD, 1990; PRATA, 1990). The quantification of the nonlinear variability, in particular, long-term trends in atmospheric total ozone is an area of intensive research, since the identification, in recent years, of the major spring-time Antarctic ozone hole and the general decreasing trend in stratospheric ozone throughout the high latitudes (BOJKOV et al., 1990; CALLIS et al., 1991). In this paper, a recently developed cell dynamical system model for atmospheric flows (MARY SELVAM 1990; MARY SELVAM et al., 1992) is summarized. The model predicts quantum-like mechanics for atmospheric flows extending up to the stratosphere and above (MEHRA et al., 1988). The model predictions are in agreement with continuous periodogram analyses of sets of twenty to hundred daily or up to 14 days non-overlapping means of atmospheric columnar total ozone content at 19 different locations.

The power spectra of atmospheric columnar total ozone follows the inverse power law form of the statistical normal distribution. Inverse power law form for the power spectra of temporal fluctuations is ubiquitous to real world dynamical systems and is a temporal signatures of self-organized criticality. (BAK, TANG and WIESENFELD, 1988) or deterministic chaos (MARY SELVAM, 1990) and implies long-

range temporal correlations. Universal quantification for self-organized criticality in the temporal fluctuations of atmospheric columnar total ozone content implies predictability of the total pattern of fluctuations. Further, trends in atmospheric total ozone may also be predictable.

2. CELL DYNAMICAL SYSTEM MODEL

In summary, (MARY SELVAM, 1990; MARY SELVAM et al., 1992) the mean flow at the planetary atmospheric boundary layer (ABL) posseses an inherent upward momentum flux of surface frictional origin. This upward momentum flux is progressively amplified by the exponential decrease of atmospheric density with height coupled with latent heat released during microscale fractional condensation by deliquescence on hygroscopic nuclei even in an unsaturated environment. This mean upward momentum flux generates helical vortex roll (or large eddy) circulations in the ABL seen as cloud rows/ streets, mesoscale cloud clusters (MCC) in the global cloud cover pattern. TOWNSEND (1956) has shown that large eddy circulations form as the spatial integration of enclosed turbulent eddies intrinsic to any turbulent shear flow. The relationship between the root mean square (r.m.s) circulations speeds W and w_* of large and turbulent

eddies of respective radii R and r is then obtained as

$$W^2 = \frac{2}{\pi}\frac{r}{R} w_*^2 \qquad (1)$$

A continuum of progressively larger eddies grow from the turbulence scale at the planetary surface with two-way ordered energy feedback between the larger and smaller scales as given in Eq.(1). Large eddy is visualized as the envelope of enclosed turbulent eddies and large eddy growth occurs in unit length step increments equal to the turbulent eddy fluctuation length r. Such a concept is analogous to the non-deterministic cellular automata computational technique where cell dynamical system growth occurs in unit length step increments during unit intervals of time (OONA and PURI 1988). Also, the concept of large eddy growth in length step increments equal to r, the turbulence length scale, i.e., length scale doubling is identified as the universal period doubling route to chaos eddy growth process. The large eddy of radius R_n at the nth stage of growth goes to form the internal circulation for the next stage, i.e., (n+1)th stage of large eddy growth. Such a concept, leads as a natural consequence, to the result that the successive values of the radii R and the r.m.s eddy circulation speeds W follow the Fibonnaci mathematical

number series, i.e., the ratio of the successive values of R (or W) is equal to Γ , the golden mean [= $(1+\sqrt{5})/2$ = 1.618].

The overall envelope of the large eddy traces a logarithmic spiral with the quasi-periodic Penrose tiling pattern for the internal structure. Atmospheric circulation structure therefore consists of a nested continuum of vortex roll circulations (vortices within vortices) with a two-way ordered energy flow between the larger and smaller scales. Such a concept is in agreement with the observed long-range spatiotemporal correlations in atmospheric flow patterns.

The cell dynamical system model also predicts the following logarithmic wind profile relationship in the ABL

$$W = (w_*/k) \ln Z \qquad (2)$$

where the Von Karman's constant **k** is identified as the universal constant for deterministic chaos and represents the steady state fractional volume dilution of large eddy by turbulent eddy fluctuations. The value of **k** is shown to be equal to $1/\Gamma^2$ (= 0.382) where Γ is the golden mean. The model predicted value of **k** is in agreement with observed values. Since the successive values of the eddy radii follow the Fibonacci mathematical number series the length scale ratio Z for the nth step of eddy growth is equal to $Z_n = R_n/r = \Gamma^n$.

Further, W represents the standard deviation of eddy fluctuations, since W is computed as the instantaneous r.m.s eddy perturbation amplitude with reference to the earlier step of eddy growth. For two successive stages of eddy growth starting from primary perturbation w_*, the ratio of the standard deviations W_{n+1} and W_n is given from Eq.(2) as (n+1)/n.

Denoting by σ , the standard deviation of eddy fluctuations at the reference level (n=1), the standard deviations of eddy fluctuations for successive stages of eddy growth are given as integer multiples of σ , i.e, σ , 2σ , 3σ , etc.,

The concept of large eddy formation as the spatial integration of enclosed turbulent eddies leads as a natural consequence to the result that the atmospheric eddy energy spectrum follows normal distribution characteristics, i.e., the square of eddy amplitude represents the eddy probability density. Incidentally, the above result, namely that the additive amplitudes of eddies when squared represent the eddy probability density is inherent to the observed sub-atomic dynamics of quantum systems and is accepted as an ad hoc assumption in quantum mechanics (MADDOX, 1988).

Atmospheric flow structure therefore follows quantum-like mechanical laws where the eddy energy spectrum represents the eddy probability

density and the apparent wave-particle duality is physically consistent in the context of atmospheric flows since the bimodal (formation and dissipation) form for energy manifestation in the bidirectional energy flow intrinsic to eddy circulations results in the formation of clouds in updrafts and dissipation of clouds in downdrafts.

The conventional power spectrum plotted as the variance versus the frequency in log-log scale will now represent the eddy probability density on logarithmic scale versus the standard deviation of the eddy fluctuations on linear scale since the logarithm of the eddy wavelength represents the the standard deviation, i.e., the r.m.s value of eddy fluctuations (Eq. 2). The r.m.s value of the eddy fluctuations can be represented in terms of statistical normal distribution as follows. A normalized standard deviation t=0 corresponds to cumulative percentage probability density equal to 50 for the mean value of the distribution. Since the logarithm of the wavelength represents the r.m.s value of eddy fluctuations the normalized standard deviation t is defined for the eddy energy distribution as $t = (\log L / \log T_{50}) - 1$ where L is the period in years and T_{50} is the period up to which the cumulative percentage contribution to total variance is equal to 50 and t=0. $\log T_{50}$ also represents the mean value for the r.m.s eddy fluctuations and is consistent with the concept of the mean level represented by r.m.s eddy fluctuations.

In the following section it is shown that continuous periodogram analyses of atmospheric total columnar ozone exhibit the signatures of quantum-like mechanics, namely, the cumulative percentage contribution to total variance, computed starting from the high frequency end of the spectrum, follows the cumulative normal distribution.

3. DATA AND ANALYSIS

Daily values of atmospheric total ozone for 19 different stations were obtained from OZONE DATA FOR THE WORLD (1987-1991). Continuous periodogram analyses (JENKINSON, 1977) was done for 30 sets of twenty to hundred daily or up to $\frac{1}{4}$ days non-overlapping averages of atmospheric total ozone content. The broadband power spectrum of total ozone time series can be computed accurately by an elementary but powerful method of analysis developed by JENKINSON (1977) which provides a quasi-continuous form of classical periodogram allowing systematic allocation of the total variance and degrees of freedom of the data series to logarithmically spaced elements of the frequency range (0.5,0). The periodogram is constituted for a fixed set of 10000(m) periodicities which increase geometrically as $L_m = 2 \exp(Cm)$ where $C = .001$ and $m = 0,1,2,...m$. The data Y_t for the N data points were used. The periodogram estimates the set of

$A_m \cos(2 \pi \nu_m t - \phi_m)$ where A_m, ν_m and ϕ_m denote respectively the amplitude, frequency and phase angle for the mth periodicity. The cumulative percentage contribution to total variance was computed from high frequency side of the spectrum. The period T_{50} at which 50% contribution to total variance occurs is taken as reference and the normalized standard deviation t_m values are computed as

$$t_m = (\log T_m / \log T_{50}) - 1$$

The power spectra are plotted in Figure 1 as cumulative percentage contribution to total variance versus the normalized standard deviation t. The statistical normal distribution is also plotted as crosses in Fig. 1 and represents the cumulative percentage probability for the normalized standard deviation t. The short horizontal lines in the lower part of the spectra indicate the lower limit above which the spectra are the same as the normal distribution as determined by the statistical chi-square test for "goodness of fit" at 95% confidence level. It is seen from Fig. 1 that the power spectra of atmospheric total ozone are the same as the statistical normal distribution when plotted in this manner. Table 1 gives the mean and standard deviation of the data, the periodicites T_{50}, T_{75}, T_{90} up to which the cumulative percentage contribution to total variance is equal to 50, 75 and 90

respectively, and the peak periodicities for dominant wave bands for which the normalized variance is equal to or more than 1.

4. DISCUSSION AND CONCLUSION

From Fig 1. it is seen that the spectra of temporal (days) fluctuations of atmospheric columnar total ozone content follow the universal and unique inverse power law form of the statistical normal distribution such that the square of the eddy amplitude represents the eddy probability density corresponding to the normalised standard deviation t_m equal to $(\log L_m/\log T_{50}) - 1$ where L_m is the period up to which the cumulative percentage contribution to total variance is equal to 50. Inverse power law form for the power spectra of temporal fluctuations is a signature of self-organized criticality in the non-linear variability of atmospheric columnar total ozone content. The unique quantification for self-organized criticality in terms of the statistical normal distribution presented in this paper implies predictability of the total pattern of fluctuations in the atmospheric total columnar ozone content over a period of time. It may therefore be possible to predict future trends in atmospheric total columnar ozone content. The applications of the above result for predictability studies will be presented in a separate paper.

The peak periodicities in the wave-bands with normalized variance equal to or more than 1 (TABLE 1) correspond to the time periods of the

quasi-periodic Penrose tiling pattern traced by internal circulations of the large eddy (see section 2) and are respectively equal to $t(2+\Gamma)=3.6t$, $t\,\Gamma(2+\Gamma)=5.8t$, $t\,\Gamma^2(2+\Gamma)=9.5t$, $t\,\Gamma^3(2+\Gamma)=15.3t$, $t\,\Gamma^4(2+\Gamma)=24.8t$ where t, the primary perturbation time period is the diurnal cycle of solar heating. The 2.2 day wave which is present in the data analysed may correspond to the period $t(2/\Gamma+1)=2.2t$ of the small scale circulation internal to primary circulation according to the concept of the eddy continuum energy structure (Eq.1). The dominant periodicities in atmospheric columnar total ozone time series may therefore be expressed as functions of the golden mean. Other studies of total ozone variability (CHANDRA, 1986; GAO and STANFORD, 1990; PRATA, 1990; DUNKERTON, 1991) also show quasi-periodicities close to those predicited by the model.

Acknowledgements-- The authors express their gratitude to Dr. A. S. R. Murty for his keen interest and encouragement during the course of this study.

REFERENCES

BAK P.C., TANG C. and WIESENFELD K. 1988 Phy. Rev. **A38**, 364.

BOJKOV R., BISHOP L., HILL W.J., REINSEL G.C. and TIAO G.C. 1990 J. geophy. Res. **95(D7)**, 9735.

CALLIS L.B., BOUGHNER R.E., NATARAJAN M., LAMBETH J.D., BAKER D. and BLAKE J.B. 1991 J. geophy. Res. **96(D2)**, 2921.

CHANDRA S. 1986 J. geophy. Res. **91(D2)**, 2719.

GAO X.H. and STANFORD J. L. 1990 J. geophy. Res. **95(D9)**, 13797.

JENKINSON A.F. 1977 A Powerful Elementary Method of Spectral Analysis for use with Monthly, Seasonal or Annual Meteorological Time Series, U.K. Meteorol. Office, Met. O. 13 Branch Memorandum No. 57, pp 23.

MADDOX J. 1988 Nature **332**, 581.

MARY SELVAM A. 1990 Can. J. Phys. **68**, 831.

MARY SELVAM A., PETHKAR J.S. and KULKARNI M.K.	1992	Int'l. J. Climatol. 12 (In press).
MEHRA P. MARY SELVAM A. and MURTHY A.S.R.	1988	Adv. Atmos. Sci.,**6(2)**, 217.
OONA Y. and PURI S.	1988	Phy. Rev. **A 38(1)** 434.
OZONE DATA FOR THE WORLD	1991	Atmospheric Environment Service, Envioronment Canada
PRATA A. J.	1990	Quart. J. Roy. Meteorol. Soc., **116(B)**, 1091.
TOWNSEND A. A.	1956	The Structure of Turbulent She Flow, Cambridge Univ. Press, U.K..
W. M. O.	1985	Atmospheric Ozone 1985 , WMO Global Ozone Research ar M nitering Project Report No. 16 Vol. I. NAS Washington D. C. 1985.

Table 1: Periodogram estimates for total ozone

Sr. No.	Station (Lat Long) (Degrees)	Time series length	Days Mean	Mean m atm-cm	Std. Dev.	T 50	T 75	T 90	Periodicities (days) contributing to maximum normalised variance (H) in the wave band H>=1				
						(Days)							
1.	Pechora (65.07N 57.96E) 1 Mar 88-8 Jun 88	50	2	426.6	42.1	15.3	41.4	91.3	7.9 85.3	8.9 -	10.7 -	14.2 -	24.7 -
2.	Pechora * 9 Jun 88-16 Sep 88	50	2	316.4	26.6	22.5	94.9	185.7	4.0 55.9	11.0 -	13.9 -	20.2 -	27.1 -
3.	Voronez * (51.40N 39.35E) 25 Aug 88-22 Dec 88	20	6	298.2	19.8	51.4	125.6	183.4	26.8	36.3	-	-	-
4.	Semipalatinsk (50.2N 80.15E) 1 Apr 88-25 Apr 88	25	1	363.6	28.9	46.5	71.1	104.9	3.7	8.9	17.1	-	-
5.	Karaganda (49.0N 74.72E) 5 Sep 88-14 Oct 88	20	2	298.8	14.1	5.2	11.3	15.9	4.0	12.2	-	-	-
6.	Alma-Ata (43.14N 76.56E) 31 May 88-7 Sep 88	20	5	323.8	20.0	35.4	116.0	186.2	18.0	25.4	37.3	-	-
7.	Cardzou (39.10N 63.30E) 1 Mar 88-6 Dec 88	20	14	307.1	22.5	99.8	362.2	554.0	51.3	66.2	90.7	-	-
8.	Dushanbe (38.35N 68.47E) 1 Apr 88-7 Sep 88	20	8	305.7	19.4	32.2	55.6	141.0	28.6	53.7	-	-	-
9.	Dushanbe 1 Apr 88-26 Nov 88	20	12	300.7	17.0	48.0	106.6	374.3	28.6	38.0	47.8	63.3	-

(contd.,)

Table 1 contd.

10. Dushanbe 9 Jul 88-26 Dec 88	20	9	299.4	16.8	54.8	89.8	189.5	24.5	29.2	53.1	82.2	-
11. Cairo (30.02N 31.15E) 1 Jan 89-1 May 89	20	6	312.8	16.3	27.9	91.4	145.9	12.9	19.9	27.3	-	-
12. Cairo 1 Mar 90-28 Jun 90	20	6	316.3	12.3	23.5	55.9	71.2	12.4	14.4	19.5	24.9	58.1
13. Aswan (24.05N 32.57E) 31 May 89-13 Sep 89	25	3	300.8	4.8	15.7	51.6	76.4	6.0 59.3	6.8 -	8.6 -	15.1 -	20.8 -
14. Poona * (18.32N 73.51E) 1 Jan 88-19 Feb 88	25	2	249.4	8.2	7.2	24.5	44.2	4.5	5.2	8.3	42.1	-
15. Poona 31 Dec 88-28 Feb 89	20	3	254.3	5.3	13.1	26.2	68.4	7.3 18.8	8.5 26.5	10.4 -	13.4 -	11.8 -
16. Bangkok * (13.44N 100.30E) 1 Jan 88-9 Apr 88	25	4	257.9	10.7	11.5	21.7	30.5	8.4	9.7	11.4	13.5	23.5
17. Bangkok 24 Apr 88-27 Aug 88	20	6	275.5	5.2	60.4	115.8	173.8	15.5	18.5	30.1	117.8	-
18. Bangkok * 6 May 89-13 Aug 89	20	5	283.3	5.6	22.1	109.3	188.8	10.0	12.7	14.7	53.3	-
19. Reykjavik (64.00N 21.30W) 1 Jul 88-19 Apr 88	25	1	344.9	20.8	7.5	24.4	40.0	3.1	3.6	5.6	-	-
20. Edmonton (53.35N 21.30W) 1 Jan 87-19 Jul 87	100	2	373.8	32.7	28.3	183.9	308.1	4.0 10.5 91.3	4.8 13.4 -	6.7 17.1 -	7.3 30.7 -	9.7 40.9 -

(condt.,)

Table 1 contd.

21. Edmonton 1 Jan 87-14 Jul 87	65	3	374.4	31.3	30.1	188.3	307.9	6.6 30.4	9.1 42.4	9.7 -	13.8 -	20.4 -
22. Goose (53.19N 60.23W) 15 May 87-28 Jul 87	75	1	368.9	27.6	12.9	84.1	133.1	2.3 7.7 35.4	3.1 8.8 -	3.4 10.2 -	4.0 12.4 -	5.8 16.1 -
23. Goose * 26 Dec 87-12 Jul 88	100	2	390.1	37.9	23.2	84.4	238.5	4.1 6.0 14.3 41.5	4.2 7.3 15.6 57.6	4.3 10.0 17.6 84.3	4.4 11.2 19.8 -	4.5 13.2 23.2 -
24. Goose 24 Feb 88-23 Jun 88	20	6	394.6	26.4	49.8	155.2	239.8	39.4	64.1	-	-	-
25. Fresno * (36.50N 120.50W) 20 Jun 88-8 Aug 88	50	1	318.3	11.4	4.8	16.8	32.1	2.6 7.9	3.1 9.6	3.5 12.1	4.7 17.0	6.7 30.8
26. Fresno 1 Jun 89-28 Sep 89	30	5	313.4	12.1	42.0	154.3	250.6	20.0	24.9	31.9	43.7	69.7
27. Hobart * (42.53S 147.21E) 1 Mar 88-8 Jun 88	100	1	279.0	13.8	11.0	44.0	117.6	2.2 3.5 11.3	2.8 4.5 19.8	2.9 5.2 40.9	3.0 8.7 -	3.2 9.8 -
28. Perth (32.00S 115.57E) 1 Apr 90-10 May 90	20	2	275.3	8.2	13.0	42.3	67.7	12.3	-	-	-	-
29. Brisbane (27.30S 153.00E) 1 Jul 88-28 Oct 88	40	3	307.3	14.8	26.7	113.2	197.9	6.5 40.4	8.9 -	10.4 -	11.9 -	28.0 -
30. Nairobi (01.18S 36.52E) 31 Mar 89-29 May 89	20	3	257.6	5.6	19.5	40.4	107.1	8.6	11.8	19.1	32.5	-

std. dev.: standard deviation of the time series.
* denotes that the data series is not distributed normally.

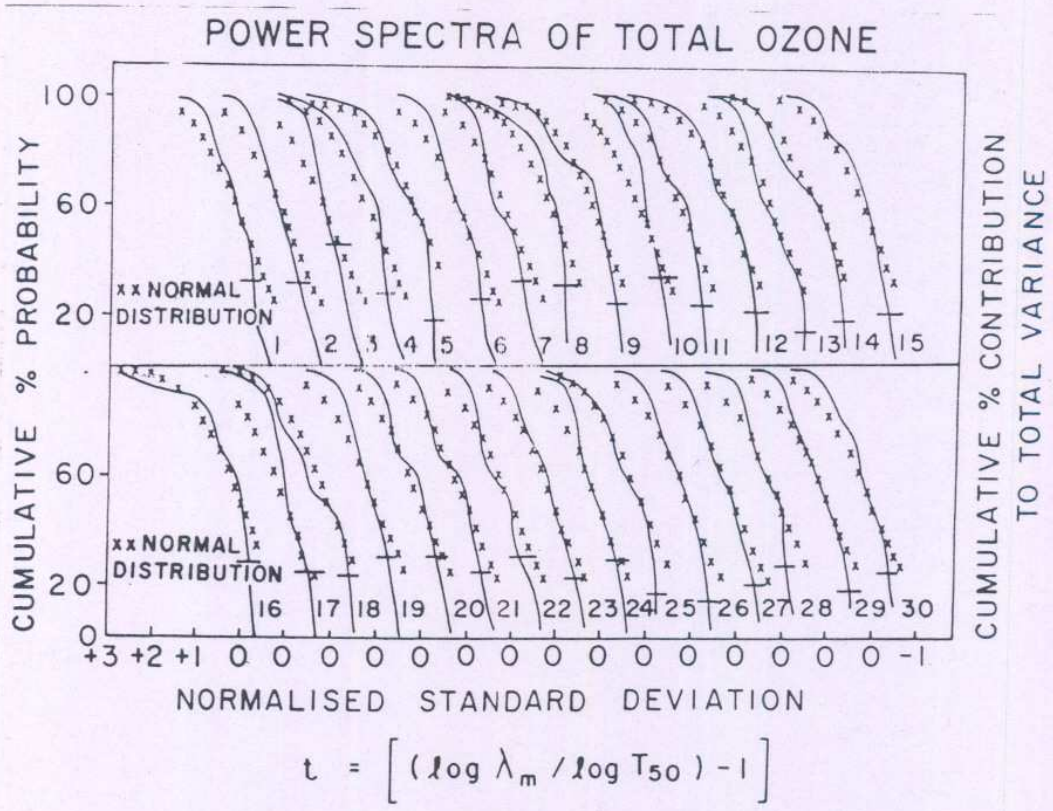

Figure 1 : Power spectra of 30 sets of atmospheric total ozone time series for 19 globally representative stations listed in Table 1.